

## Resistance to a Protein Farnesyltransferase Inhibitor in *Plasmodium falciparum*\*

Received for publication, December 2, 2004, and in revised form, January 11, 2005  
Published, JBC Papers in Press, January 20, 2005, DOI 10.1074/jbc.M413556200

Richard T. Eastman‡, John White‡, Oliver Hucke§¶, Kevin Bauer¶, Kohei Yokoyama\*\*,  
Laxman Nallan§\*\*, Debopam Chakrabarti‡‡, Christophe L. M. J. Verlinde§, Michael H. Gelb§\*\*,  
Pradipsinh K. Rathod‡\*\*§§, and Wesley C. Van Voorhis‡¶¶¶

From the Departments of ‡Pathobiology, §Biochemistry, ¶Medicine, and \*\*Chemistry, University of Washington, Seattle, Washington 98195 and the ‡‡Department of Molecular Biology and Microbiology, University of Central Florida, Orlando, Florida 32826

The post-translational farnesylation of proteins serves to anchor a subset of intracellular proteins to membranes in eukaryotic organisms and also promotes protein-protein interactions. Inhibition of protein farnesyltransferase (PFT) is lethal to the pathogenic protozoa *Plasmodium falciparum*. Parasites were isolated that were resistant to BMS-388891, a tetrahydroquinoline (THQ) PFT inhibitor. Resistance was associated with a 12-fold decrease in drug susceptibility. Genotypic analysis revealed a single point mutation in the  $\beta$  subunit in resistant parasites. The resultant tyrosine 837 to cysteine alteration in the  $\beta$  subunit corresponded to the binding site for the THQ and peptide substrate. Biochemical analysis of Y837C-PFT demonstrated a 13-fold increase in BMS-388891 concentration necessary for inhibiting 50% of the enzyme activity. These data are consistent with PFT as the target of BMS-388891 in *P. falciparum* and suggest that PFT inhibitors should be combined with other antimalarial agents for effective therapy.

Malaria causes about 300 million infections annually.<sup>1</sup> Approximately 90% of the deaths occur in Africa, with falciparum malaria a major contributor. For decades, malaria chemotherapy has relied on a limited number of drugs. Acquisition and spread of resistance to these drugs is largely responsible for a recent increase in malaria-related mortality (2, 3). This increasing burden caused by drug-resistant parasites has led investigators to seek out novel antimalarial drug targets. Among these are enzymes necessary for cellular division and differentiation. Previous work has demonstrated that the en-

zyme protein farnesyltransferase (PFT)<sup>2</sup> is a viable drug target for pathogenic protozoa, including the malaria parasite *Plasmodium falciparum* (4–8).<sup>3</sup> PFT inhibitors (PFTIs) have been developed by the pharmaceutical industry because of their anti-cancer properties (9–11). Utilizing this existing resource, we have been able to demonstrate that low nanomolar concentrations of tetrahydroquinoline (THQ)-based PFTIs inhibit *P. falciparum* PFT (PfPFT) and are cytotoxic to parasites both *in vitro* and *in vivo*.<sup>3</sup>

PFT in eukaryotic cells catalyzes the transfer of a 15-carbon isoprenoid lipid unit, a farnesyl group, from farnesyl pyrophosphate (FPP) to the C terminus of a specific set of proteins, including the Ras superfamily G-proteins (12). In addition to the Ras superfamily proteins, which are involved in the cell cycle, another protein that has been shown to be farnesylated is CENP-E, a centromere-associating protein, which plays a critical role in cell cycle progression during the M-phase (13). However, the identification of farnesylated proteins in *P. falciparum* and their role in mediating PFTI toxicity are currently under investigation.

Because of the enzymatic nature of the drug target, we have begun to investigate potential *P. falciparum* resistance to PFTIs. The THQ PFTI used in this work, BMS-388891 (Fig. 1), is a potent inhibitor of parasite proliferation and causes severe defects in maturation.<sup>3</sup> In addition, when parasites were treated with BMS-388891 and the farnesylated proteins were labeled with [<sup>3</sup>H]farnesol, there was a significant decrease in labeled 37–75-kDa proteins.<sup>3</sup>

Using a *P. falciparum* clone prone to the acquisition of drug resistance (14), we describe the selection of *P. falciparum* parasites resistant to BMS-388891 and present genetic and enzymological analyses of these parasites. We analyze the native PFT enzyme of the parent and resistant clones and demonstrate that an amino acid substitution is responsible for PFTI resistance. In addition, using the solved crystal structure of the mammalian protein farnesyltransferase, we created a model for the *P. falciparum* PFT enzyme that explains the THQ-PFT binding interactions and explains the molecular mechanism of resistance (15–18) to better facilitate drug development. Our work demonstrates PFT as the target for THQ PFTIs and provides a tool for further characterization of the PFT enzyme

\* This work was supported by the W. M. Keck Foundation Center on Microbial Pathogens at the University of Washington, Medicines for Malaria Venture, and National Institutes of Health Grants AI26912 and AI60360 (to P. K. R.) and AI054384 (to M. H. G.). The costs of publication of this article were defrayed in part by the payment of page charges. This article must therefore be hereby marked “advertisement” in accordance with 18 U.S.C. Section 1734 solely to indicate this fact.

The nucleotide sequence(s) reported in this paper has been submitted to the GenBank™/EBI Data Bank with accession number(s) AY880030, AY880031, AY880032, AY880033, and AY880034.

¶ Fellow of the German Academy of Natural Scientists Leopoldina (BMBF-LPD 9901/8-77).

§§ Senior Scholar in Global Infectious Diseases, Ellison Medical Foundation.

¶¶¶ To whom correspondence should be addressed: Dept. of Medicine, University of Washington, 1959 N.E. Pacific, Seattle, WA 98195-7185. Tel.: 206-543-2447; Fax: 206-685-8681; E-mail: wesley@u.washington.edu.

<sup>1</sup> www.mmv.org (2004).

<sup>2</sup> The abbreviations used are: PFT, protein farnesyltransferase; THQ, tetrahydroquinoline; PFTI, protein farnesyltransferase inhibitor; PfPFT, *P. falciparum* PFT; FPP, farnesyl pyrophosphate; WT, wild type.

<sup>3</sup> Nallan, L., Bauer, K. D., Bendale, P., Rivas, K., Yokoyama, K., Hornèy, C. M., Pendyala, P. R., Floyd, D., Lombardo, L. J., Williams, D. K., Hamilton, A., Sebti, S., Windsor, W. T., Weber, P. C., Buckner, F. S., Chakrabarti, D., Gelb, M. H., and Van Voorhis, W. C. (2005) *J. Med. Chem.*, in press.

TABLE I  
Primers used for sequencing PfPFT  $\alpha$  and  $\beta$  subunit genes

Using the *P. falciparum* 3D7 protein farnesyltransferase  $\alpha$  and  $\beta$  genomic sequences as a template, primers to amplify and sequence the *P. falciparum* Dd2 PFT  $\alpha$  and  $\beta$  genes were constructed. The location of the primer relative to the start is given in parentheses.

Primer	Sequence
PFT $\alpha$ subunit sense primers	
PfPFT (Start)	AACCCATGGAAAATCGATGCTTG
PfPFT (560)	ATCTATATTGAGGAGGGG
PfPFT (1090)	TATAATAATTCATTGTGGG
PFT $\alpha$ subunit antisense primers	
PfPFT (595)	TATTATCTATATTTTTCCCC
PfPFT (1120)	GTATAAAATATCTATATACCC
PfPFT (End)	GCCCAACATAAAATATCATATTG
PFT $\beta$ subunit sense primers	
PfPFT (Start)	GATATGAGGAGTTTTAACCATGGAAAAATGATTCGTATTTATTG
PfPFT (455)	CAAGTAGATTGTTCCATG
PfPFT (1030)	GAAACGGAAGAATATAACG
PfPFT (1522)	CACATTGCAACGACTTATG
PfPFT (2110)	AAGAGAATGAAATAAAGG
PfPFT (2640)	CTATATAATATCACAGTTG
PFT $\beta$ subunit antisense primers	
PfPFT (550)	ATATTTTTTCACATATATCTTC
PfPFT (1000)	TCAAAAGTATGTAAGGTG
PfPFT (1570)	AAAAGTTATTTTCTTCATCAT
PfPFT (2160)	AGTTTATATCCTTTTCACTAC
PfPFT (End)	CCAGATCTTTTATTTTCATCTTTGTAGTAAC

in an effort to develop this as a target of antimalarial chemotherapy.

#### EXPERIMENTAL PROCEDURES

**Parasites**—Experiments described in this study were performed with a clone of *P. falciparum* Dd2 strain parasites, which is derived from clone W2 (14). Parasites were cultured in an asynchronous manner *in vitro* using standard conditions and media (19). Parasites from infected erythrocytes were isolated for PFT enzyme extraction by treatment with 0.1% (w/v) saponin.

**Selection of BMS-38891-resistant Parasites**—Selection of resistant parasites was conducted as described previously (14, 20). Briefly, triplicate 30-ml cultures with a 2% hematocrit and  $10^8$  infected red blood cells of an isogenic, recently cloned population of *P. falciparum* Dd2 (WT) were challenged with varying concentrations of THQ BMS-38891 (300, 100, 33.3, 11.1, and 3.7 nM) in the culture medium. In addition, triplicate flasks were inoculated with 10 parasites as a growth control to gauge when limiting numbers of parasites would appear by microscopy. The medium was changed every other day, maintaining the initial drug concentration, and fresh red blood cells were added once per week. Cultures were maintained under continuous drug pressure for 80 days. Giemsa-stained blood smears of cultures were used to detect parasite outgrowth, and a 2% infected red blood cell level was considered positive. Clonal isolates of resistant parasites from drug-challenged cultures were generated by limiting dilutions.

**Proliferation Assays,  $ED_{50}$** —*In vitro* responses to the THQ PFTI were calculated from 72-h [ $^3$ H]hypoxanthine incorporation assays as described previously (21, 22). Incorporation of [ $^3$ H]hypoxanthine into nucleic acids was measured using a Chameleon liquid scintillation counter (Hidex, Turku, Finland). The ability of the PFTI to reduce the parasite growth was reported as an  $ED_{50}$  value, the effective dose of PFTI that reduces the hypoxanthine incorporation by 50%, compared with the untreated positive control after subtraction of a no parasite background control.

**Genetic Analysis**—Genomic DNA was isolated from the parasites using standard phenol/chloroform protocols. Duplicate independent PCR reactions for both the PFT  $\alpha$  and  $\beta$  subunits were amplified using the Expand high fidelity polymerase PCR System (Roche Applied Science). These amplicons were ligated into the pGEM<sub>T</sub> cloning vector (Promega, Madison, WI), and five *Escherichia coli* transformants derived from each PCR reaction were sequenced. Sequencing results were analyzed using Vector NTI Suite 9.0 (Invitrogen). Primers used to amplify and sequence the PFT subunits in *P. falciparum* Dd2 are given in Table I.

**Protein Farnesyltransferase Assay and Determination of  $IC_{50}$** —PfPFT was partially purified from the isolated parasites by ammonium

sulfate fractionation and Q-Sepharose chromatography from parasite lysates as described by Chakrabarti *et al.* (5, 23). Peak fractions were concentrated using a Vivaspin 15R concentrator according to the manufacturer's recommendations (Vivascience, Hannover, Germany). Assays for PfPFT activity were performed with a PFT-specific scintillation proximity assay kit (Amersham Biosciences) slightly modified from the one described previously (23).<sup>3</sup> One  $\mu$ M biotinylated lamin B peptide substrate (biotin-YRASNRSICAIM) was used. The concentration of [ $^3$ H]farnesyl pyrophosphate (FPP) (3.7 MBq) was increased beyond the manufacturer's recommendations to 1  $\mu$ M to ensure that the enzyme substrate was in excess of its likely  $K_m$  value (the  $K_m$  of farnesyl diphosphate for human PFT is  $9.3 \pm 5.8$  nM) (24). Increasing the FPP concentration to 2  $\mu$ M had no effect on the amount of the product formed (data not shown). All reactions were performed in triplicate. Controls (no enzyme reaction values) were subtracted from experimental values before calculation of percent inhibition. The effectiveness of the PFTI is reported as an  $IC_{50}$  value, the concentration of inhibitor that reduces the activity of the enzyme by 50% compared with the untreated positive control.

**Determination of  $K_m$  for the Peptide Substrate**—Determination of the  $K_m$  value for the peptide substrate of the PFT enzyme was conducted using the scintillation proximity assay as described above. The FPP substrate concentration was 1  $\mu$ M, whereas the peptide substrate concentrations used were 0, 0.25, 0.5, 1, 2, 3, 4, and 5  $\mu$ M. Each experiment was repeated in duplicate for both the WT and mutant enzymes. Control values obtained from reactions with no peptide substrate were subtracted from the experimental values. The experimental values were graphed as velocity as determined by counts per min obtained as a function of peptide substrate concentration. These values were fitted to a Michaelis-Menten plot using Prism 3.0 (Graphpad, San Diego, CA).

**Determination of the  $K_i$  Values for BMS-38891**— $K_i$  values of BMS-38891 for both the WT and mutant native PFT enzyme were obtained by non-linear regression fit of percent inhibition *versus* inhibitor concentration at fixed peptide substrate concentration (1  $\mu$ M). The  $K_m$  values for the WT and Y837C enzyme were used to obtain the value of  $K_i$  for the PFTI by fitting the observed rate data from the  $IC_{50}$  experiments as a function of inhibitor concentration at constant peptide substrate concentration by non-linear regression. In Equation 1,  $V_i/V_0$  is the ratio of enzyme activity in the presence of inhibitor over the activity without inhibitor,  $S$  is the peptide substrate concentration,  $K_m$  is the value determined for each enzyme (see Table II), and  $I$  is the concentration of BMS-38891.

$$V_i/V_0 = ([S] + K_m)/([S] + K_m(1 + [I]/K_i)) \quad (\text{Eq. 1})$$

**Homology Modeling of PfPFT**—The program MODELLER (25), version 6v2, was used for the creation of the homology model of PfPFT. The

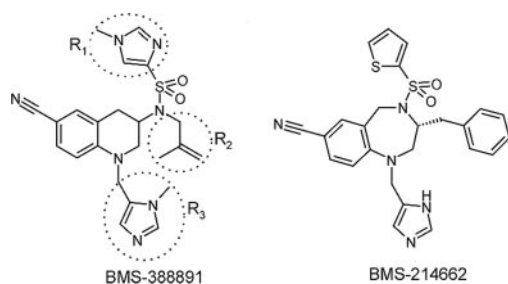


FIG. 1. The structures of the tetrahydrobenzodiazepine BMS-214662 and of the THQ BMS-388891. The binding mode of BMS-214662 to rat PFT has been revealed in a recent x-ray structure (17). BMS-388891 is the *Pf*PFT inhibitor discussed here. The nomenclature of the substituents of the THQ used throughout the text is indicated.

crystal structure of rat PFT complexed with the non-substrate tetrapeptide inhibitor CVFM and FPP was used as the template structure (Protein Data Bank file 1JCR (18)). The sequences of the two subunits of *Pf*PFT were obtained from the PlasmoDB data base (www.plasmodb.org, Gene loci: PFL2050w for  $\alpha$  and chr11.glm\_528 for  $\beta$ ). A BLAST search resulted in 14  $\alpha$ - and 12  $\beta$ -subunit sequences. They were aligned with the program T-COFFEE (26). The pairwise sequence alignment used for the homology modeling was extracted from this multiple alignment. Only regions with reasonable reliability of the alignment were included. The model of *Pf*PFT comprises the following sequence segments (throughout the text corresponding residue numbers of rat PFT are given in parentheses; these also correspond to the residue numbers of human PFT):  $\alpha$ : 72–164 (Rat $\alpha$ 87–179), 300–411 (Rat $\alpha$ 184–283);  $\beta$ : 421–677 (Rat $\beta$ 71–315), 806–896 (Rat $\beta$ 330–417). The levels of sequence identity (similarity) between *Pf*PFT and rat PFT in these regions amount to 23% (53%) for the  $\alpha$ -subunit and 37% (56%) for the  $\beta$ -subunit. The catalytic zinc ion, six structurally conserved water molecules (Protein Data Bank water residue numbers in 1JCR: 1163, 1167, 1170, 1241, 1573, 1181), and FPP were included in the model. The conformation of FPP was considered to be flexible during the model calculations. For this purpose parameters for FPP were added to the MODELLER force field using the lipid parameters of the “charmm27” force field (27). 20 different models of *Pf*PFT were calculated. The model with the lowest value of the objective function of MODELLER was used for further work. The model of the mutant Tyr- $\beta$ 837 to Cys was obtained by replacing tyrosine with cysteine and selecting the lowest energy rotamer with INSIGHTIII (version 97.0; Accelrys Inc.).

**Ligand Docking Calculations**—The program FLO (version 6.02) (28) was used for the docking of BMS-388891, which contains a sulfonamide functional group (Fig. 1). Most sulfonamide nitrogens show significant deviations from planarity, *i.e.* they are pyramidalized (29). The  $N_M$  atom type of FLO takes this into account but does not allow for the inversion of the sulfonamide nitrogen during Monte Carlo conformational searches. To consider the inversion, both stereochemical configurations of this nitrogen were considered in separate calculations. Thus, to account for both configurations of the chiral carbon atom and of the sulfonamide nitrogen, four docking calculations were necessary. The initial placements of the four stereochemical configurations of BMS-388891 were obtained by modifying the structure of BMS-214662, a tetrahydrobenzodiazepine (Fig. 1), as observed in the x-ray structure with rat PFT (17) after superpositioning this structure on the *Pf*PFT homology model. 2000 cycles of Metropolis Monte Carlo conformational searches were performed for each starting configuration of BMS-388891 in the *Pf*PFT binding site employing the MCDOCK module of the FLO program. A distance restraint was introduced for the bond between the imidazole nitrogen and the zinc ion.

## RESULTS

**BMS-388891-resistant *P. falciparum* Clones Can Be Selected**—Earlier studies demonstrated that *P. falciparum* 3D7 was highly sensitive to growth inhibition by the THQ PFTI, BMS-388891, with an  $ED_{50}$  of 7.0 nM.<sup>3</sup> To determine whether resistance to BMS-388891 could occur, a one-step selection protocol was used employing varying concentrations of BMS-388891. We employed a recently cloned Dd2 strain, which is prone to the acquisition of drug resistance (14). In cultures treated with 100 nM BMS-388891, two of three flasks developed parasite growth by day 21. Flasks with inhibitor concentrations

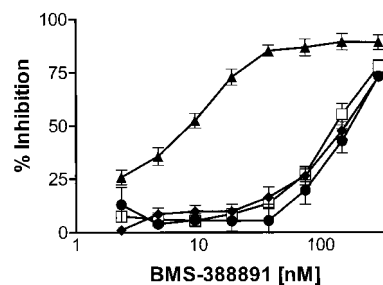


FIG. 2. Growth inhibition by BMS-388891 of *P. falciparum* WT and resistant clones G7, H7, and B10. Shown is an *in vitro* growth inhibition assay, using [<sup>3</sup>H]hypoxanthine uptake as a measure of proliferation. Results are shown as percent growth inhibition as a function of BMS-388891 inhibition concentration. *P. falciparum* Dd2 WT ( $\blacktriangle$ ), *P. falciparum* Dd2 Y837C clones G7 ( $\blacklozenge$ ), H7 ( $\bullet$ ), and B10 ( $\square$ ). Shown are the mean of multiple replicates and standard deviation.

of 33.3, 11.1, or 3.7 nM and the no drug 10 parasite control flasks all had demonstrable parasites by day 11. In contrast, after 80 days of continuous culturing the remaining flask challenged with 100 nM BMS-388891 and all of the flasks challenged with 300 nM BMS-388891 remained negative for parasites. Clonal parasites were derived from the populations of the two 100-nM flasks in which parasite outgrowth occurred, and these clones were used for further experimentation. Growth rate of the drug-resistant clones with or without drug pressure did not differ significantly from the WT population without drug pressure (data not shown).

**BMS-388891-resistant Clones Show 12-Fold Resistance**—Resistant clones obtained from the two 100-nM BMS-388891-treated flasks showed altered  $ED_{50}$  values compared with the WT clone, which had an  $ED_{50}$  of 10 nM. Clonal isolates obtained from the drug selection had an  $ED_{50}$  value of 105 nM (clone B10), 110 nM (clone G7), and 120 nM (clone H7), a 12-fold increase in resistance to the inhibitor (Fig. 2).  $ED_{50}$  experiments were conducted multiple times (WT,  $n = 5$ ; G7,  $n = 4$ ; H7,  $n = 7$ ; B10,  $n = 3$ ). Student's *t* test demonstrated significance between the  $ED_{50}$  values of the WT and each resistant clone ( $p < 0.01$ ). These clonal isolates retained identical  $ED_{50}$  values after 6 weeks of culture without drug pressure (data not shown). Thus the BMS-388891 resistance phenotype in these clones is stable in the absence of drug pressure.

**A Single Amino Acid Substitution Causes the Resistance Phenotype**—To identify the basis of resistance, both the  $\alpha$  and  $\beta$  genes of PFT from all three resistant clones and the WT clone were sequenced. Only a single nucleotide difference in the  $\beta$  PFT gene was found between the parent and the resistant clones, resistant clones being 100% identical. Multiple *E. coli* transformants from independent PCRs were used for sequencing to rule out PCR-induced errors. The single point mutation was a transition from an adenine to a guanine in the  $\beta$  gene. This mutation altered the predicted amino acid coding of the  $\beta$  subunit at position 837 from a tyrosine to a cysteine. Fig. 3 shows a fragment of the predicted amino acid alignment of the PFT  $\beta$  subunit from *P. falciparum* Dd2 WT, *P. falciparum* Dd2 Y837C mutant clone (all three clones have identical nucleotide sequence), and the human sequence (NCBI accession number P49356). Of note, by sequencing the cDNA we can infer the presence of an intron near the 3'-end of the PFT  $\alpha$  (data not shown, GenBank<sup>TM</sup> accession number AY880030). This intron is not currently noted in either the NCBI or PlasmoDB database.

**Mutant *Pf*PFT Has a Decreased Affinity for BMS-388891 and Has an Increased Affinity for Peptide Substrate**—The  $IC_{50}$  value for PFT enzyme extracted from the *P. falciparum* Dd2 WT clone was 0.7 nM. This is similar to the value that was found previously for *P. falciparum* 3D7 (0.6 nM).<sup>3</sup> However, the

*P. falciparum* WT 830 PKERIDYHTC 840  
*P. falciparum* Y837C 830 PKERIDYHTC 840  
 Human 354 PGKSRDFHTC 364

FIG. 3. Predicted location of the altered residue in the mutant PFT  $\beta$  subunit. A partial amino acid alignment comparing the predicted sequences of *P. falciparum* Dd2 wild type, *P. falciparum* Dd2 Y837C mutant, and the human PFT  $\beta$  subunits.

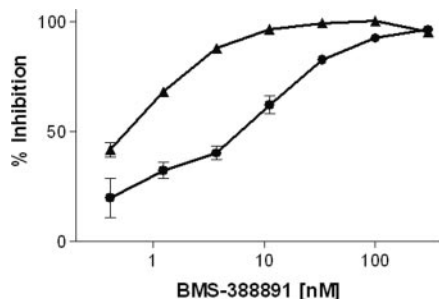


FIG. 4. BMS-388891 inhibition of PFT enzyme from the parent clone and resistant clone H7. Using the native PFT enzyme isolated from both *P. falciparum* Dd2 WT ( $\blacktriangle$ ) and Y837C mutant clone H7 ( $\bullet$ ), the percent enzyme inhibition as a function of BMS-388891 inhibitor concentration was determined. Shown are the mean values and standard deviation of multiple experiments.

mutant PFT enzyme extracted from resistant clone H7 had an  $IC_{50}$  value against BMS-388891 of 9 nM, 13-fold higher than the WT enzyme (Fig. 4). This is almost identical to the 12-fold shift seen in the  $ED_{50}$  value comparing WT and resistant isolates. This correlation implicates the alteration of the PFT enzyme as the cause for the observed drug resistance of the parasite and thus demonstrates that the mechanism of action of the THQ class of PFT inhibitors is by direct interaction and inhibition of the PFT enzyme.  $IC_{50}$  experiments for both the WT enzyme and the Y837C mutant enzyme were conducted three times with a Student's *t* test demonstrating  $p < 0.01$ , a statistically significant difference.

The  $K_m$  values of both WT and the Y837C mutant PFT enzyme for the peptide substrate YRASNRSICAIM is listed in Table II. The values from the calculation of BMS-388891  $K_i$  values for both WT and the Y837C enzyme are shown in Table II. The mutated enzyme has a higher affinity for the peptide substrate (lower  $K_m$ ) and also reduced the binding affinity of BMS-388891 (higher  $K_i$ ). Together these alterations allow the mutant PFT enzyme to function in the presence of higher concentrations of PFTI compared with the WT PFT enzyme.

Of note, this class of PFTIs has displayed little to no selectivity for the *P. falciparum* PFT enzyme compared with the mammalian PFT enzyme (data not shown). This lack of selectivity is supported by the homology model (see below).

**Homology Model of P/PFT**—The homology model of P/PFT reveals that despite the relatively low overall level of sequence identity (see under "Experimental Procedures"), many of the residues contacting BMS-214662 in mammalian PFT are conserved (17). Five conservative substitutions of the surface residues in proximity of the inhibitor are obvious. Residues in rat PFT with a side chain atom within 7 Å from BMS-214662 that are replaced in P/PFT (RatPFT→P/PFT) are: Tyr- $\beta$ 93 → Leu- $\beta$ 443 (3.6 Å), Cys- $\beta$ 95 → Ser- $\beta$ 445 (4.5 Å), Tyr- $\alpha$ 166 → Phe- $\alpha$ 151 (4.8 Å), Phe- $\beta$ 360 → Tyr- $\beta$ 836 (5.5 Å), Ala- $\alpha$ 129 → Ser- $\alpha$ 114 (6.1 Å) (Fig. 5). The conformation of the FPP molecule, which contributes to the surface contacting BMS-214662, was left unchanged by MODELLER.

**Docking of BMS-388891**—The best predicted binding mode of BMS-388891 to wild-type P/PFT was obtained for the (*S*)-enantiomer. It shows high similarity to the binding mode of BMS-214662 (Fig. 5); the root mean square deviation of the

TABLE II  
 Difference in affinity of the Y837C mutant PFT enzyme for peptide substrate and BMS-388891

Clone <sup>a</sup>	$K_m$	$K_i^b$
	$\mu M$	nM
<i>P. falciparum</i> Dd2 WT	$0.64 \pm 0.12$	$0.22 \pm 0.01$
<i>P. falciparum</i> Dd2 Y837C	$0.32 \pm 0.1$	$1.2 \pm 0.2$

<sup>a</sup> The YRASNRSICAIM peptide substrate  $K_m$  values for both the *P. falciparum* Dd2 WT and Y837C mutant enzyme isolated from clone H7 as determined using the Michaelis-Menten plot of activity as a function of peptide substrate concentration.

<sup>b</sup> The  $K_i$  values of WT and Y837C mutant *P. falciparum* PFT enzyme were determined by fitting the  $IC_{50}$  data as a function of inhibitor concentration at constant peptide substrate concentration [ $1 \mu M$ ] by non-linear regression. All results are given as the mean  $\pm$  S.D. of three experimental replicates.

cyano-phenyl group and the adjacent carbon and nitrogen atoms of the saturated ring and of the zinc-binding R3 groups (Fig. 1) amounts to 1.2 Å. The BMS-388891 R2 fills the pocket occupied by the benzyl substituent of BMS-214662. The pocket is partly formed by the side chain of Tyr- $\beta$ 837[Rat $\beta$ 361], but only one of the two terminal carbon atoms of R2 is contacting this side chain. Both sulfonamide oxygen atoms are solvent accessible. One of them is located at a distance of 3.5 Å from the  $NH_2$  side chain nitrogen atom of Arg- $\beta$ 564[Rat $\beta$ 202], suggesting that minor changes of the position of this side chain might allow for the formation of a hydrogen bond. In fact, minimization of the ligand in the docked orientation considering the side chain conformation of Arg- $\beta$ 564[Rat $\beta$ 202] as flexible, lead to formation of this hydrogen bond (N–O distance: 3.0 Å). The arginine side chain shows a slight shift toward the sulfonamide group upon the minimization, whereas the ligand position remains unchanged. The imidazole attached to the  $SO_2$  group ( $R_1$  in Fig. 1) is contacting the phenyl ring of Phe- $\alpha$ 151[RatTyr- $\alpha$ 166] in an edge to face orientation. The 16 best predicted ligand binding positions show a highly conserved placement of R2, whereas the position of R1 shows variability. However, in most cases the edge to face orientation of R1 with the Phe- $\alpha$ 151 phenyl ring is maintained. The best predicted binding energy for the WT enzyme is  $-21.1$  kJ/mol. (Note that the association energy contributed by the binding of the imidazole nitrogen atom to the zinc ion is not considered by the docking program.)

The BMS-388891 binding mode predicted for the Y837C mutant of P/PFT shows a nearly identical position of the ring system and the zinc binding moiety as well as highly similar locations of the sulfonamide substituents (Fig. 5). The change of the shape of the R2 pocket by the mutation leads to a shift of R2 toward the side chain of the newly introduced cysteine. The position of the terminal carbon of the R2 group that is contacting the Tyr- $\beta$ 837 side chain in the wild type changes by about 2.4 Å. The score for the best predicted binding mode in the mutant binding site is  $-15.4$  kJ/mol, which is 5.7 kJ/mol higher than the wild-type enzyme. This apparent increase in binding energy would be expected with the increased  $K_i$  for the inhibitor as observed experimentally.

## DISCUSSION

Here we report the first instance of parasites with resistance to PFTIs. These parasites have increased resistance to PFTIs, specifically BMS-388891, a THQ. The only observed amino acid substitution was Y837C in the  $\beta$  subunit of PFT. This mutation affects both the enzyme affinity for the peptide substrate and the THQ inhibitor, which likely contribute to the drug-resistant phenotype. These resistant clones, obtained from two independently cultured flasks, are identical to the WT parent clone except for the Y837C mutation.

Experimental results using the PFT enzyme purified from

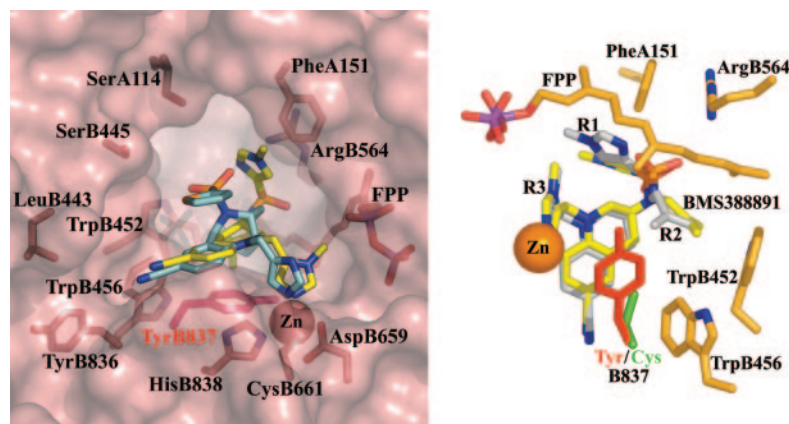


FIG. 5. **Predicted binding mode of BMS-388891 to the *PfPFT* enzyme.** *Left*, superposition of the best predicted binding mode for BMS-388891 (yellow carbon atoms) with BMS-214662 (light blue carbons) as bound to rat PFT. Residues that contribute to the contact surface of the inhibitors or that are within 7 Å from BMS-214662 and that are not conserved between rat and *PfPFT* (see Homology Model of *PfPFT* under “Results”) are specified. *Right*, superposition of the binding modes of BMS-388891 as predicted for WT *PfPFT* (yellow carbon atoms) and the Y837C mutant (gray carbon atoms). The side chain of Cys-β837 is shown in green. From this perspective the slightly changed location of R2 in the mutant enzyme is evident. (Figure prepared with PyMol (DeLano Scientific, San Carlos, CA).)

the WT clone and a resistant clone revealed that the  $K_m$  value for the peptide substrate in the Y837C mutated enzyme is decreased by half. In addition, the Y837C mutated enzyme demonstrates reduced binding affinity for BMS-388891, as demonstrated by a 6-fold increase in the  $K_i$  value of BMS-388891 for the Y837C *versus* the WT enzyme. The combination of the 2-fold increase in affinity for the peptide substrate and the 6-fold decreased affinity for BMS-388891 likely contributes to the 13-fold increase in the  $IC_{50}$  of the Y837C mutant enzyme.

Mutagenesis studies of the yeast and human PFT enzyme have provided clues to the impact of altering residues which have proximity to the catalytic zinc ion (30–32). Del Villar *et al.* (32) demonstrated that alteration of the homologous residue in the human PFT enzyme, Tyr-β361 (corresponding to *PfPFT* β837) to Leu, plays a critical role in peptide substrate binding and resistance to tricyclic inhibitors (Schering-Plough PFT inhibitors SCH44342 and SCH56582). In addition, the Del Villar study (32) demonstrates that this alteration alters the affinity for peptide substrates. Our finding that the  $K_m$  was decreased in the Y837C mutant relative to the WT *PfPFT* is consistent with this residue being in proximity to the binding site of the peptide substrate in *PfPFT*.

Findings with the PFT mutants are supported by determination of the three-dimensional crystal structure of the mammalian PFT enzyme (15, 16, 18). Specifically, the crystal structure of the mammalian PFT bound to BMS-214662, a tetrahydrobenzodiazepine PFTI related to the THQ series, demonstrates the striking interaction between the aromatic ring structure of the PFTI and the aromatic ring of RatTyr-β361 (17).

The good agreement of the predicted binding mode of BMS-388891 with the binding geometry of BMS-214662 reflects the structural similarity of these inhibitors and the high degree of conservation of the binding site region relevant for the binding of BMS-214662. The difference in binding energy of BMS-388891 with the mutation Y837C amounts to 4.3 kJ/mol (calculated with  $\Delta G = -RT \ln K_i$ , with the  $K_i$  of the WT enzyme being 0.22 nM and that of the Y837C enzyme 1.2 nM; see Table II). This is in good agreement with the predicted binding energy difference of 5.7 kJ/mol.

According to the scoring function of FLO, the mutation leads to a lower energy conformation of the THQ PFTI in the binding site; the ligand strain for BMS-388891 drops from 9.2 to 2.2 kJ/mol. However, this only partly compensates a loss of favorable van der Waals interactions. The van der Waals energy

(computed as the sum of the van der Waals and the contact energy terms of the FLO force field) of the mutant complex is 11.4 kJ/mol higher than that of the wild-type complex. This can mainly be ascribed to the superior fit of the planar tyrosine side chain against the bicyclic ring system of the inhibitor. In the x-ray structure with BMS-214662 the cyano-phenyl group of the inhibitor is found in a favorable parallel-displaced orientation with respect to the aromatic ring of RatTyr-β361 (17). The predicted binding mode of BMS-388891 to *PfPFT* shows the cyano-phenyl group in a highly similar position relative to the homologous residue Tyr-β837 (Fig. 5). The association free energy of benzene in aqueous solution has been reported to be -6.3 kJ/mol (33). This value is close to the binding free energy difference of BMS-388891 between the WT *PfPFT* enzyme and the Y837C mutant. This suggests that, in agreement with what was indicated by the different contributions to the FLO score, the loss of the favorable interaction between the cyano-phenyl and the aromatic ring of the Tyr side chain is the major reason for the observed effect of the Tyr replacement by Cys. Thus, the effect of this mutation on the binding energy of other THQs, given that they adopt the same binding mode, is expected to be highly similar.

One might argue that the mutation Y837C could affect the geometry and/or the electronic properties of the zinc system leading to impaired binding of BMS-388891 solely because of less favorable interaction of R3 with the zinc ion. As in the mammalian enzyme, the phenyl ring of the Tyr-β837 side chain, RatTyr-β361, is in van der Waals contact with the zinc-coordinating His-β838[Ratβ362] and Cys-β661[Ratβ299]. Further, the oxygen atom of the Tyr-β837 side chain is located at a distance of only 3.2 Å from the sulfur atom of Cys-β661 suggesting the presence of a hydrogen bond. However, the replacement of the homologous residue, Tyr-β361, by Leu in the mammalian PFT does not appreciably affect the affinity for the tetrapeptide substrates CIIM, CIIC, and CIIA (32). Thus, a potential hydrogen bond to the sulfur atom of the zinc binding cysteine does not appear to have an appreciable effect on the ligand binding properties of the zinc ion. The finding that no significant change of the geometry of the zinc system is observed in the recent related structure of GGTase I, where a Leu replaces the Tyr corresponding to Tyr-β837[Ratβ361] (34), further supports the assumption that the mutation Y837C does also not affect the geometry of the zinc system.

Our finding that a single amino acid substitution can shift the sensitivity of *PfPFT* by 13-fold demonstrates the liability of

enzyme inhibitors for malaria therapy. It is estimated that an infected individual with a 2% parasitemia harbors  $\sim 10^{11}$  parasites (1). We have demonstrated that the Y837C mutation can arise independently at least twice in  $3 \times 10^8$  parasites. This suggests that this mutation could arise multiple times in each infected individual. This, however, does not negate the potential use of this or other enzyme inhibitors as chemotherapeutic agents for malaria. It is likely that THQ PFTIs, as well as other antimalarials, will need to be combined with other agents to achieve cures and to decrease the occurrence of drug resistance.

**Acknowledgments**—We thank Karthikeyan Ganesan, Lynn K. Barrett, Kasey L. Rivas, and Carrie M. Hornèy for technical support and David M. Floyd, David K. Williams, and Louis J. Lombardo of the Bristol-Myers Squibb Co. for providing the original THQ PFTIs, advice on THQ synthetic chemistry, and intensive support of our PFTI program.

## REFERENCES

- Rathod, P. K. (2001) in *Antimalarial Chemotherapy: Mechanisms of Action, Resistance, and New Directions in Drug Discovery* (Rosenthal, P. J., ed) Humana Press, Totowa, NJ
- May, J., and Meyer, C. G. (2003) *Trends Parasitol.* **19**, 432–435
- White, N. J. (2004) *J. Clin. Investig.* **113**, 1084–1092
- Buckner, F. S., Eastman, R. T., Nepomuceno-Silva, J. L., Speelman, E. C., Myler, P. J., Van Voorhis, W. C., and Yokoyama, K. (2002) *Mol. Biochem. Parasitol.* **122**, 181–188
- Chakrabarti, D., Azam, T., DelVecchio, C., Qiu, L. B., Park, Y., and Allen, C. M. (1998) *Mol. Biochem. Parasitol.* **94**, 175–184
- Ohkanda, J., Lockman, J. W., Yokoyama, K., Gelb, M. H., Croft, S. L., Kendrick, H., Harrell, M. I., Feagin, J. E., Blaskovich, M. A., Sebti, S. M., and Hamilton, A. D. (2001) *Bioorg. Med. Chem. Lett.* **11**, 761–764
- Ohkanda, J., Buckner, F. S., Lockman, J. W., Yokoyama, K., Carrico, D., Eastman, R., Luca-Fradley, K., Davies, W., Croft, S. L., Van Voorhis, W. C., Gelb, M. H., Sebti, S. M., and Hamilton, A. D. (2004) *J. Med. Chem.* **47**, 432–445
- Wiesner, J., Kettler, K., Sakowski, J., Ortmann, R., Katzin, A. M., Kimura, E. A., Silber, K., Klebe, G., Jomaa, H., and Schlitzer, M. (2004) *Angew. Chem. Int. Ed. Engl.* **43**, 251–254
- Bell, I. M. (2004) *J. Med. Chem.* **47**, 1869–1878
- Haluska, P., Dy, G. K., and Adjei, A. A. (2002) *Eur. J. Cancer* **38**, 1685–1700
- Sebti, S. M., and Adjei, A. A. (2004) *Semin. Oncol.* **31**, 28–39
- Yokoyama, K., Goodwin, G. W., Ghomashchi, F., Glomset, J., and Gelb, M. H. (1992) *Biochem. Soc. Trans.* **20**, 489–494
- Abrieu, A., Kahana, J. A., Wood, K. W., and Cleveland, D. W. (2000) *Cell* **102**, 817–826
- Rathod, P. K., McErlean, T., and Lee, P. C. (1997) *Proc. Natl. Acad. Sci. U. S. A.* **94**, 9389–9393
- Duntzen, P., Kammlott, U., Crowther, R., Weber, D., Palermo, R., and Birktoft, J. (1998) *Biochemistry* **37**, 7907–7912
- Park, H. W., Boduluri, S. R., Moomaw, J. F., Casey, P. J., and Beese, L. S. (1997) *Science* **275**, 1800–1804
- Reid, T. S., and Beese, L. S. (2004) *Biochemistry* **43**, 6877–6884
- Long, S. B., Hancock, P. J., Kral, A. M., Hellinga, H. W., and Beese, L. S. (2001) *Proc. Natl. Acad. Sci. U. S. A.* **98**, 12948–12953
- Trager, W., and Jensen, J. B. (1976) *Science* **193**, 673–675
- Rathod, P. K., Khosla, M., Gassis, S., Young, R. D., and Lutz, C. (1994) *Antimicrob. Agents Chemother.* **38**, 2871–2876
- Desjardins, R. E., Canfield, C. J., Haynes, J. D., and Chulay, J. D. (1979) *Antimicrob. Agents Chemother.* **16**, 710–718
- Jiang, L., Lee, P. C., White, J., and Rathod, P. K. (2000) *Antimicrob. Agents Chemother.* **44**, 1047–1050
- Chakrabarti, D., Da Silva, T., Barger, J., Paquette, S., Patel, H., Patterson, S., and Allen, C. M. (2002) *J. Biol. Chem.* **277**, 42066–42073
- Omer, C. A., Kral, A. M., Diehl, R. E., Prendergast, G. C., Powers, S., Allen, C. M., Gibbs, J. B., and Kohl, N. E. (1993) *Biochemistry* **32**, 5167–5176
- Sali, A., and Blundell, T. L. (1993) *J. Mol. Biol.* **234**, 779–815
- Notredame, C., Higgins, D. G., and Heringa, J. (2000) *J. Mol. Biol.* **302**, 205–217
- Feller, S. E., Gawrisch, K., and MacKerell, A. D., Jr. (2002) *J. Am. Chem. Soc.* **124**, 318–326
- McMartin, C., and Bohacek, R. S. (1997) *J. Comput. Aided Mol. Des.* **11**, 333–344
- Ohwada, T., Okamoto, I., Shudo, K., and Yamaguchi, K. (1998) *Tetrahedron Lett.* **39**, 7877–7880
- Kral, A. M., Diehl, R. E., deSolms, S. J., Williams, T. M., Kohl, N. E., and Omer, C. A. (1997) *J. Biol. Chem.* **272**, 27319–27323
- Mitsuzawa, H., Esson, K., and Tamanoi, F. (1995) *Proc. Natl. Acad. Sci. U. S. A.* **92**, 1704–1708
- Del Villar, K., Urano, J., Guo, L., and Tamanoi, F. (1999) *J. Biol. Chem.* **274**, 27010–27017
- Jorgensen, W. L., and Severance, D. L. (1990) *J. Am. Chem. Soc.* **112**, 4768–4774
- Taylor, J. S., Reid, T. S., Terry, K. L., Casey, P. J., and Beese, L. S. (2003) *EMBO J.* **22**, 5963–5974